

Generation of macroscopic entanglement in ensemble systems based on silicon vacancy centers

Jian-Zhuang Wu(武建壮), Ying Xi(奚滢), Bo-Ya Li(李博雅), Lian-E Lu(芦连娥), and Yong-Hong Ma(马永红)

Citation: Chin. Phys. B, 2024, 33 (**9**): 090308. DOI: 10.1088/1674-1056/ad5d93
Journal homepage: http://cpb.iphy.ac.cn; http://iopscience.iop.org/cpb

What follows is a list of articles you may be interested in

Delayed-measurement one-way quantum computing on cloud quantum computer

Zhi-Peng Yang(杨智鹏), Yu-Ran Zhang(张煜然), Fu-Li Li(李福利), and Heng Fan(范桁)
Chin. Phys. B, 2024, 33 (**9**): 090304. DOI: 10.1088/1674-1056/ad6253

Detecting the quantum phase transition from the perspective of quantum information in the Aubry-André model

Geng-Biao Wei(韦庚彪), Liu Ye(叶柳), and Dong Wang(王栋)
Chin. Phys. B, 2024, 33 (**7**): 070301. DOI: 10.1088/1674-1056/ad2f1f

Quantum circuit-based proxy blind signatures: A novel approach and experimental evaluation on the IBM quantum cloud platform

Xiaoping Lou(娄小平), Huiru Zan(昝慧茹), and Xuejiao Xu(徐雪娇)
Chin. Phys. B, 2024, 33 (**5**): 050307. DOI: 10.1088/1674-1056/ad22d5

Quantum correlations and entanglement in coupled optomechanical resonators with photon hopping via Gaussian interferometric power analysis

Y. Lahlou, B. Maroufi, and M. Daoud
Chin. Phys. B, 2024, 33 (**5**): 050303. DOI: 10.1088/1674-1056/ad2a6e

Complementary monogamy and polygamy properties among multipartite systems

Tao Li(李陶), Jing-Yi Zhou(周静怡), Qi Sun(孙琪), Zhi-Xiang Jin(靳志祥), Deng-Feng Liang(梁登峰), and Ting Luo(罗婷)
Chin. Phys. B, 2024, 33 (**3**): 030305. DOI: 10.1088/1674-1056/ad1748

Generation of macroscopic entanglement in ensemble systems based on silicon vacancy centers

Jian-Zhuang Wu(武建壮), Ying Xi(奚滢), Bo-Ya Li(李博雅),
Lian-E Lu(芦连娥), and Yong-Hong Ma(马永红)†

School of Science, Inner Mongolia University of Science and Technology, Baotou 014010, *China*

(Received 7 May 2024; revised manuscript received 11 June 2024; accepted manuscript online 2 July 2024)

Entanglement in macroscopic systems, as a fundamental quantum resource, has been utilized to propel the advancement of quantum technology and probe the boundary between the quantum and classical realms. This study focuses on a unique hybrid quantum system comprising of an ensemble of silicon vacancy (SiV) centers coupled to phononic waveguides in diamond via strain interactions. By employing two sets of time-dependent, non-overlapping driving fields, we investigate the generation process and dynamic properties of macroscopic quantum entanglement, providing fresh insights into the behavior of such hybrid quantum systems. Furthermore, it paves the way for new possibilities in utilizing quantum entanglement as an information carrier in quantum information processing and quantum communication.

Keywords: quantum entanglement, silicon vacancy centers, diamond waveguide

PACS: 03.67.Bg, 61.72.–y **DOI:** 10.1088/1674-1056/ad5d93

1. Introduction

Entanglement, as a most notable and unique feature of quantum mechanics, plays a critical role in testing foundational quantum mechanics and has been applied successively to the quantum technology sector, including quantum computing, remote quantum cryptography, and the enhancement of quantum measurement sensitivity.[1–4] The early study on quantum entanglement was mainly concerned with microscopic systems composed of a small number of particles. However, as an effective way to explore the quantum-to-classical transition, the possibility of entanglement existing in macroscopic systems has been a central question in fundamental debates.[5–7] Over the past decade, entanglement in macroscopic (many-body) physical systems has attracted widespread interest.[8–15] At present, various theoretical and experimental schemes for creating entanglement at the macroscopic level have been realized experimentally.[16–18]

Recently, macroscopic entanglement in solid-state systems attracts more and more attention because electrons' spins in solid-state systems exhibit longer relaxation times,[19] higher controllability, greater storage capacity, and the ability to transmit quantum information.[20–24] Numerous experiments demonstrated the existence of macroscopic entanglement, such as entanglement between superconducting circuits[25,26] and between nuclear spin qubits.[3,27,28]

However, in experiments, the generation of macroscopic entanglement is quite challenging due to the decoherence effects . Hybrid quantum systems comprising SiV centers may be promising candidates to generate macroscopic entanglement because of their versatile quantum properties. Recently, a number of schemes to generate different quantum states were proposed in SiV systerms. For instance, Lemonde *et al*. proposed an effective method for coupling SiV centers in diamond waveguides with propagating phonons for quantum network applications.[29] Chen *et al*. investigated the preparation of stable spin squeezed states in SiV centers via microwave fields within diamond waveguides.[30] A hybrid quantum system integrating SiV centers into phononic modes of diamond waveguides was proposed to achieve various types of spin interactions via microwave driving.[31] To our knowledge, the generation of macroscopic entanglement in such hybrid systems has not yet been studied.

In this paper, we explore the generation of macroscopic entanglement between two spin clusters within a hybrid quantum system composing of an ensemble of SiV centers. By formulating an effective Hamiltonian and employing the master equation, we conduct a theoretical examination of the macroscopic entanglement generation between the two spin clusters. Through numerical simulations, we scrutinize the specific impact of various parameters on the generation and duration of quantum entanglement. Key parameters influencing the generation of macroscopic entanglement, such as the detuning Δ_s, decoherence rate γ_s, coupling constant λ_1, and the characteristic time of environmental dissipation Γ_{eff}, are thoroughly explored. Our investigation aims to elucidate how these parameters collectively shape the entanglement process between the two spin clusters, offering a theoretical foundation for more precise experimental manipulation of quantum entanglement.

†Corresponding author. E-mail: myh_dlut@126.com

© 2024 Chinese Physical Society and IOP Publishing Ltd

2. Model

We consider a spin-phonon hybrid system containing two separated SiV centers coupled to the same phononic modes of a one-dimensional diamond waveguide through strain-induced interactions, as shown in Fig. 1(a). N_1 and N_2 SiV centers are located in sections S_1 and S_2 of a diamond waveguide, respectively. We first consider SiV centers in section S_1 which is driven by two time-dependent microwave fields $\Omega_1(t)$ and $\Omega_2(t)$. The Hamiltonian of this system can be expressed as[29,31,32]

$$H_{S_1} = H_{\mathrm{SiV}_{S_1}} + H_{\mathrm{ph}} + H_{\mathrm{strain}_{S_1}}, \tag{1}$$

where $H_{\mathrm{SiV}_{S_1}}$ represents the Hamiltonian of SiV centers in section S_1; H_{ph} denotes the Hamiltonian of the phonon modes; $H_{\mathrm{strain}_{S_1}}$ describes the strain-induced coupling between the orbital degrees of freedom of SiV centers in section S_1 and the resonant phononic modes of the waveguide, as shown in Fig. 1(b). The dynamics of SiV centers are described by the Hamiltonian $H_{\mathrm{SiV}_{S_1}}$ as follows:[29,31,32]

$$\begin{aligned} H_{\mathrm{SiV}_{S_1}} = \sum_{j=1}^{N_1} \Big[& \omega_{\mathrm{B}} |2\rangle_j \langle 2| + \Delta |3\rangle_j \langle 3| + (\omega_{\mathrm{B}} + \Delta) |4\rangle_j \langle 4| \\ & + \frac{\Omega_1(t)}{2} |1\rangle_j \langle 4| \, \mathrm{e}^{\mathrm{i}\omega_1 t} \\ & + \frac{\Omega_2(t)}{2} |2\rangle_j \langle 3| \, \mathrm{e}^{\mathrm{i}\omega_2 t} + \mathrm{H.c.} \Big], \end{aligned} \tag{2}$$

where ω_{B} represents the energy level splitting caused by the Zeeman effect, and we set $\omega_{\mathrm{B}} = 2\pi \times 5$ GHz.[32,33] The ground state of SiV centers is fourfold degenerate, with the corresponding energy level splitting $\Delta = 2\pi \times 46$ GHz. Two time-independent microwave fields $\Omega_{1,2}(t)$ with frequencies $\omega_{1,2}$ induce transitions from state $|1\rangle$ to $|4\rangle$ and $|2\rangle$ to $|3\rangle$, respectively. The Hamiltonian of phonon modes H_{ph} can be written as

$$H_{\mathrm{ph}} = \sum_{n,k} \omega_{n,k} a^{\dagger}_{n,k} a_{n,k}, \tag{3}$$

where $a_{n,k}$ and $a^{\dagger}_{n,k}$ correspond to the annihilation and creation operators for the phonon modes, respectively. Considering the strain-induced coupling between SiV centers in segment S_1 and phonon modes in the microwave waveguide within the framework of linear elastic theory, the Hamiltonian $H_{\mathrm{strain}_{S_1}}$ can be expressed as[29,33]

$$H_{\mathrm{strain}_{S_1}} \approx \sum_{n,k} \left[g_{n,k} j_+ a_{n,k} + g^{*}_{n,k} j_- a^{\dagger}_{n,k} \right], \tag{4}$$

where the operator j_+ denotes the spin-conserving raising operator, while j_- represents the corresponding lowering operator. For a small quasi-1D (one-dimensional) diamond acoustic waveguide, the length, width, and thickness can be chosen as $L \sim 10$ μm–100 μm, w, $d \leq 200$ nm^2, respectively, and it has the group velocity $v \sim 1 \times 10^4$ m/s. The parameter $g_{n,k}$ signifies the coupling strength, typically falling within the range of $2\pi \times (4 \sim 14)$ MHz.[29,34,35] Considering that the phonon modes of the small-scale waveguide exhibit significant frequency separation ($\Delta\omega_n \geq 2\pi \times 50$ MHz), we can simplify the treatment by regarding the mechanical mode as a single standing wave with a frequency of approximately $\omega_n \simeq 2\pi \times 46$ GHz.[30] Subsequently, the Hamiltonian described in Eq. (1) can be reformulated as

$$\begin{aligned} H_{\mathrm{SiV}_{S_1}} = \sum_{j}^{N_1} \Big[& \omega_{\mathrm{B}} |2\rangle_j \langle 2| + \Delta |3\rangle_j \langle 3| + (\omega_{\mathrm{B}} + \Delta) |4\rangle_j \langle 4| \\ & + \frac{\Omega_1(t)}{2} |1\rangle_j \langle 4| \, \mathrm{e}^{\mathrm{i}\omega_1 t} + \frac{\Omega_2(t)}{2} |2\rangle_j \langle 3| \, \mathrm{e}^{\mathrm{i}\omega_2 t} + \mathrm{H.c.} \Big] \\ & + \omega_n a^{\dagger} a + \sum_{j}^{N_1} \left[g^j_n (|3\rangle_j \langle 1| + |4\rangle_j \langle 2|) a + \mathrm{H.c.} \right]. \end{aligned} \tag{5}$$

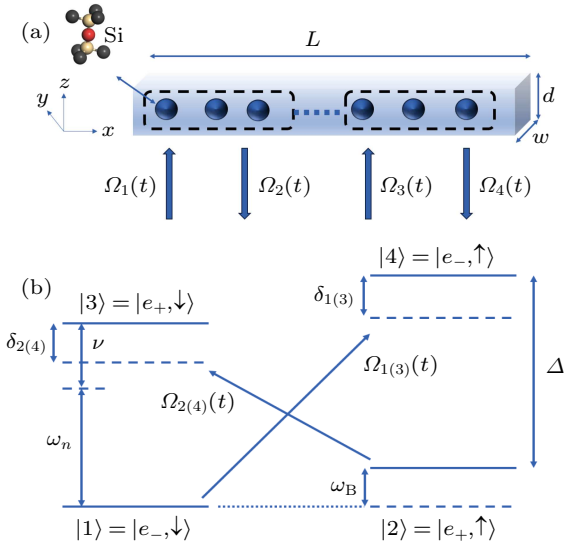


Fig. 1. (a) Sketch of an array of SiV centers embedded in a one-dimensional (1D) diamond waveguide. The length, width, and thickness of the waveguide are L, w, d, respectively. Molecular structure of the SiV center is shown as the inset. (b) The level structure of the electronic ground state of the SiV center. The time-dependent microwave driving fields induce the transitions between levels $|1\rangle \leftrightarrow |4\rangle$ and $|2\rangle \leftrightarrow |3\rangle$, while the transitions between levels $|1\rangle \leftrightarrow |3\rangle$ and $|2\rangle \leftrightarrow |4\rangle$ are caused by the strain-induced coupling.

By employing a unitary transformation $U = \mathrm{e}^{-\mathrm{i}H_0 t}$ to simplify the system Hamiltonian with

$$H_0 = \sum_j [(\omega_n - \omega_2) |2\rangle_j \langle 2| + \omega_n |3\rangle_j \langle 3| + \omega_1 |4\rangle_j \langle 4| + \omega_n a^{\dagger} a],$$

the Hamiltonian $H_{\mathrm{SiV}_{S_1}}$ for the silicon vacancy centers in segment S_1 is rewritten as

$$\begin{aligned} H_{\mathrm{SiV}_{S_1}} = \sum_{j}^{N_1} \Big[& (\nu - \delta_2) |2\rangle_j \langle 2| + \nu |3\rangle_j \langle 3| + \delta_1 |4\rangle_j \langle 4| \\ & + \frac{\Omega_1(t)}{2} |1\rangle_j \langle 4| + \frac{\Omega_2(t)}{2} |2\rangle_j \langle 3| \\ & + g^j_n (|3\rangle_j \langle 1| + |4\rangle_j \langle 2|) a \, \mathrm{e}^{\mathrm{i}\Delta'_1 t} + \mathrm{H.c.} \Big], \end{aligned} \tag{6}$$

where ν, δ_1, and δ_2 represent the detunings corresponding to the specific frequencies $\omega_{n,k}$, ω_1, and ω_2, as well as the detunings associated with the characteristic frequencies of states $|3\rangle$ and $|4\rangle$. The condition $\Delta_1' = \omega_1 + \omega_2 - \omega_n$ is crucial for ensuring energy conservation. When the detunings $\delta_{1,2}$ are significantly larger than the driving frequencies $\Omega_{1,2}$ (i.e., $\delta_{1,2} \gg \Omega_{1,2}$), the system can be further simplified via the Froehlich–Nakajima transformation to remove the direct dependency on the high-energy states $|3\rangle$ and $|4\rangle$.[36–38] This transformation serves as an effective technique for handling the high-energy states within the system by confining the dynamics to lower energy levels, thereby streamlining the analysis of quantum systems. Consequently, we derive an equivalent two-level Hamiltonian

$$\begin{aligned} H_{\mathrm{SiV}_{S_1}} =& \sum_j^{N_1} \left[\varepsilon_1 |2\rangle_j \langle 2| + \lambda_1 a |2\rangle_j \langle 1| \right. \\ &\left. + \Lambda_1 a |1\rangle_j \langle 2| \, \mathrm{e}^{\mathrm{i}\Delta_1'} + \mathrm{H.c.}\right], \end{aligned} \tag{7}$$

where the parameters ε_1, λ_1, and Λ_1 are given as

$$\begin{aligned} \varepsilon_1 &= \nu - \delta_2 - \frac{\Omega_2^2}{4\delta_2} + \frac{\Omega_1^2}{4\delta_1}, \\ \lambda_1 &= -\left(\frac{1}{\nu} + \frac{1}{\delta_2}\right)\frac{\Omega_2 g_n}{4}, \\ \Lambda_1 &= -\left(\frac{1}{\delta_1} + \frac{1}{\delta_1 + \delta_2 - \nu}\right)\frac{\Omega_1 g_n}{4}. \end{aligned} \tag{8}$$

In the following sections, we consider the total mixed system comprising sections $S_{1,2}$, connected through a common phonon mode. The effective Hamiltonian for this mixed system is written as

$$\begin{aligned} H =& \frac{\varepsilon_1}{2} J_{1z} + \lambda_1 a J_{1+} + \Lambda_1 a J_{1-} \, \mathrm{e}^{\mathrm{i}\Delta_1' t} \\ &+ \frac{\varepsilon_2}{2} J_{2z} + \lambda_2 a J_{2+} + \Lambda_2 a J_{2-} \, \mathrm{e}^{\mathrm{i}\Delta_2' t} + \mathrm{H.c.}, \end{aligned} \tag{9}$$

where the operators

$$\begin{aligned} J_{1z,2z} &= \sum_{j=1}^{N_{1,2}} (|2\rangle_j \langle 2| - |1\rangle_j \langle 1|), \\ J_{1+,2+} &= \sum_{j=1}^{N_{1,2}} |2\rangle_j \langle 1|, \\ J_{1-,2-} &= \sum_{j=1}^{N_{1,2}} |1\rangle_j \langle 2| \end{aligned}$$

are collective spin operators of silicon vacancy centers, with subscripts 1 and 2 denoting the two parts and N_1, N_2 being the total number of spins in respective silicon vacancy center sections. Moreover, the parameters ε_2, λ_2, and Λ_2 are defined as

$$\begin{aligned} \varepsilon_2 &= \nu - \delta_4 - \frac{\Omega_4^4}{4\delta_4} + \frac{\Omega_3^2}{4\delta_3}, \\ \lambda_2 &= -\left(\frac{1}{\nu} + \frac{1}{\delta_4}\right)\frac{\Omega_4 g_n}{4}, \\ \Lambda_2 &= -\left(\frac{1}{\delta_3} + \frac{1}{\delta_3 + \delta_4 - \nu}\right)\frac{\Omega_3 g_n}{4}. \end{aligned}$$

By adjusting the microwave fields, we effectively set $\varepsilon_1 = -\varepsilon_2 = \Delta_\mathrm{s}$, indicating that these two parts of the silicon vacancy centers are physically distinct. Assuming the setup operates at a temperature of 100 mK,[39,40] where the phonon number of the acoustic mode approaches 0, i.e., $\langle a^\dagger a \rangle \approx 0$. Under the condition $\Delta_\mathrm{s} \gg \lambda_{1,2} g_n, \Lambda_{1,2} g_n$ applying the gauge transformation $H \to \mathrm{e}^{-S} H_\mathrm{eff} \mathrm{e}^{S}$ with[38,41]

$$\begin{aligned} S =& \frac{1}{\Delta_\mathrm{s}} g_n \left[\lambda_1 (a^\dagger J_{1-} - a J_{1+}) + \Lambda_1 (a J_{1-} - a^\dagger J_{1+}) \right. \\ &\left. + \lambda_2 (a J_{2+} - a^\dagger J_{2-}) + \Lambda_2 (a^\dagger J_{2+} - a J_{2-})\right], \end{aligned} \tag{10}$$

we can obtain an effective projected Hamiltonian within the spin ensemble subspace[41,42]

$$\begin{aligned} H_\mathrm{eff} =& \frac{\Delta_\mathrm{s}}{2} J_1^z - \frac{\Delta_\mathrm{s}}{2} J_2^z + \frac{1}{\Delta_\mathrm{s}} \\ &\times \left\{\lambda_1^2 J_1^+ J_1^- - \lambda_2^2 J_2^+ J_2^- - \Lambda_1^2 J_1^- J_1^+ + \Lambda_2^2 J_2^- J_2^+ \right. \\ &\left. + (\lambda_1 \Lambda_2 - \lambda_2 \Lambda_1)(J_1^+ J_2^+ + J_1^- J_2^-)\right\}. \end{aligned} \tag{11}$$

To include spin relaxation induced by mechanical dissipation in the model, the dynamical evolution of this system can be described by the quantum master equation

$$\begin{aligned} \frac{\mathrm{d}\rho(t)}{\mathrm{d}t} =& -\mathrm{i}\left[H_\mathrm{eff}, \rho\right] + (n_\mathrm{th} + 1)\Gamma_\mathrm{eff} D\left[J_{1-}\right]\rho(t) \\ &+ n_\mathrm{th}\Gamma_\mathrm{eff} D\left[J_{1+}\right]\rho(t) + \gamma_\mathrm{s} D\left[J_{1z}\right]\rho(t) \\ &+ (n_\mathrm{th} + 1)\Gamma_\mathrm{eff} D\left[J_{2-}\right]\rho(t) \\ &+ n_\mathrm{th}\Gamma_\mathrm{eff} D\left[J_{2+}\right]\rho(t) + \gamma_\mathrm{s} D\left[J_{2z}\right]\rho(t), \end{aligned} \tag{12}$$

where n_th is the average phonon number, and the superoperator $D[\hat{o}]\hat{\rho} = \hat{o}\hat{\rho}\hat{o}^\dagger - \frac{1}{2}\hat{o}^\dagger\hat{o}\hat{\rho} - \frac{1}{2}\hat{\rho}\hat{o}^\dagger\hat{o}$ is the standard Lindblad superoperator. $\Gamma_\mathrm{eff} = \Gamma_\mathrm{m} \cdot (\lambda_{1,2}/\Delta_\mathrm{s})^2$ represents the collective spin relaxation caused by the mechanical dissipation Γ_m of the corresponding acoustic modes.

In our research, we explore the phenomenon of macroscopic quantum entanglement between two ensembles of SiV centers using numerical methods. In the related experimental setup, the quantum variables of interest are the collective spins' projections of the SiV center samples in two specific directions, analogous to the classical position and momentum variables. To be specific, if we set the spin of the SiV center samples along the direction of the x-axis, by introducing quantum commutation relations akin to the classical commutation relations $[J_z, J_y] = \mathrm{i}J_x$, i.e., $[X, P] = \mathrm{i}$ where $X = J_z/\sqrt{J_x}$ and $P = J_y/\sqrt{J_x}$. We can define X and P as the normalized projections of spin on the z and y axes, respectively. Consequently, our model predicts correlations in the collective spins of the

two samples in the y and z directions. For the evaluation of entanglement, we apply the criterion[43,44]

$$\xi = \frac{\mathrm{Var}(J_{1y}+J_{2y})+\mathrm{Var}(J_{1z}+J_{2z})}{|\langle J_{1x}\rangle|+|\langle J_{2x}\rangle|}, \tag{13}$$

where $\mathrm{Var}(\cdots)$ represents the statistical variance. $\xi < 1$ signifies the presence of quantum entanglement between the two macroscopic spin ensembles. To achieve this entangled state, we initialize one ensemble in a coherent spin state (CSS)[17,18] along the x axis and the other ensemble in a CSS along the $-x$ axis, while ensuring that the expectation values and related variances in the y and z directions satisfy specific conditions, i.e., $\langle J_{1x}\rangle = J$, $\langle J_{2x}\rangle = -J$, $\langle J_{iy}\rangle = \langle J_{iz}\rangle = \langle C_{iyz}\rangle = 0$, and $\langle J_{iy}^2\rangle = \langle J_{iz}^2\rangle = J/2$ $(i = 1,2)$. This strategy was initially proposed and implemented in the experimental entanglement of two macroscopic atomic samples.[17] Through optical pumping and microwave spin manipulation techniques, we can similarly prepare CSS states for SiV center spin ensembles. Based on the ξ value defined in the above formula, the computation of this metric involves solving a system of linear equations to guarantee that the experimental conditions fulfill the prerequisites for generating entanglement.

3. Results and discussion

Based on the exact solutions of Eqs. (A1)–(A14) in Appendix A, the effects of parameters Δ_s, γ_s, λ_1, and Γ_{eff} on the entanglement between two macroscopic atomic sample are analyzed.

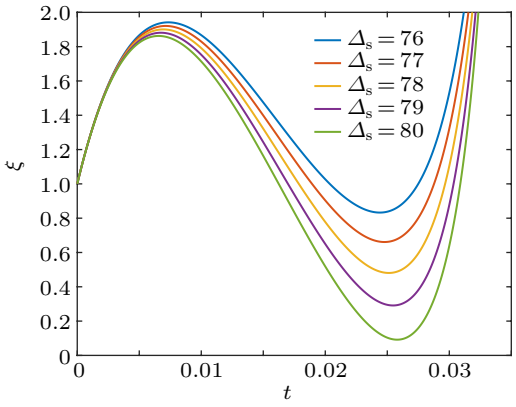


Fig. 2. Evolution of entanglement ξ over time with different parameters Δ_s. The correlation parameters are $\lambda_1 = \lambda_2 = 0.1$, $\Lambda_1 = \Lambda_2 = 2.5$, $N = 25$, $n_{\mathrm{th}} = 100$, $\Gamma_{\mathrm{eff}} = 0.120$, and $\gamma_s = 0.1$.

Figure 2 illustrates the evolution of macroscopic quantum entanglement over time under different detuning conditions (Δ_s). Initially, the entanglement measure (ξ) is greater than 1, indicating the absence of entanglement in the system. As time evolution, entanglement characteristics in the system begin to appear, as it takes a certain amount of time to form two independent ensembles of SiV centers. This time duration is related to the coupling strength, as shown in Fig. 4. Increasing Δ_s from 76 to 80 extends the duration of entanglement, while the maximum value of ξ will decrease. Additionally, higher values of Δ_s reduce the time required for entanglement formation, suggesting that larger Δ_s values are advantageous for rapidly generating macroscopic entanglement. The effective Hamiltonian of the system is derived under the condition that Δ_s is much greater than $\lambda_{1,2}g_n$. It is observed that entanglement forms only under larger Δ_s conditions, consistent with the observed phenomena. This indicates that by appropriately adjusting the Δ_s parameter, we can effectively manipulate the system to produce the desired quantum entanglement. This manipulation is crucial for implementing efficient quantum information processing and quantum computing protocols.

Figure 3 illustrates the evolution of macroscopic quantum entanglement over time under different decoherence rates γ_s (0.1, 0.4, 0.7, 1.0, and 1.3). The results clearly show that as the value of γ_s increases, the degree of entanglement in the system gradually diminishes. Furthermore, a higher decoherence rate leads to a narrower time window during which the system maintains a macroscopic entangled state (i.e., $\xi < 1$), indicating a delay in the entanglement generation process while an earlier attainment of the maximum entanglement degree. Additionally, as γ_s increases, the maximum achievable entanglement degree decreases, reflected in the increased minimum value of ξ. γ_s represents the spin state decoherence rate, signifying the speed at which spin state coherence is lost due to environmental noise or other non-ideal factors. At lower γ_s levels, the system can sustain coherence for longer periods, beneficial for preserving and enhancing the degree of quantum entanglement. Conversely, higher γ_s values result in rapid spin state decoherence, leading to a swift entanglement reduction. The main reason is that quantum entanglement heavily depends on the quantum state coherence, and the decoherence process disrupts this superposition state, thereby weakening the entanglement. In scenarios with elevated γ_s, environmental interference with the quantum state intensifies, prompting the quantum system towards a mixed state rather than a pure state, diminishing its entanglement capacity.

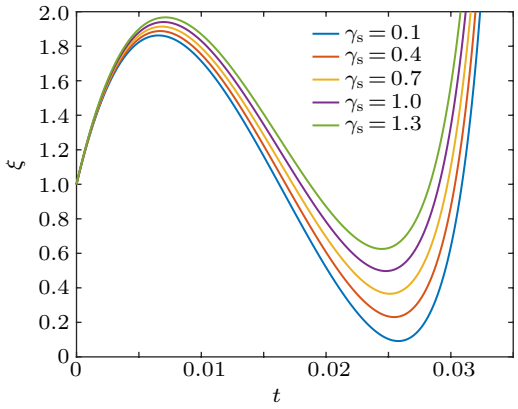


Fig. 3. Evolution of entanglement ξ over time with different parameters γ_s. The correlation parameters are $\lambda_1 = \lambda_2 = 0.1$, $\Lambda_1 = \Lambda_2 = 2.5$, $N = 25$, $n_{\mathrm{th}} = 100$, $\Gamma_{\mathrm{eff}} = 0.120$ and $\Delta_s = 80$.

From the analysis of Fig. 4, it is evident that an increase in the coupling constant λ_1 results in a faster decrease for the entanglement measure ξ, leading to the system reaching a quantum entangled state more rapidly (i.e., $\xi < 1$). This observation underscores the significant role of strong coupling (i.e., higher values of (λ_1)) in hastening the process of entanglement formation. Specifically, when λ_1 is raised from 1 to 3, the time taken for ξ to fall below 1 in the system is notably reduced. This highlights how the intensity of the coupling term in the Hamiltonian directly impacts the speed at which quantum entanglement is established between the spin ensembles. With an increased coupling term λ_1, the quantum interactions facilitating entanglement unfold within a shorter temporal framework, causing ξ to swiftly drop below the critical threshold of 1.

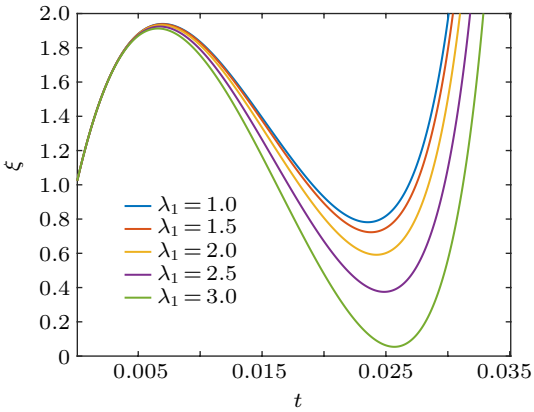


Fig. 4. Evolution of entanglement ξ over time with different parameters λ_1. The correlation parameters are $\Delta_s = 80$, $\Lambda_1 = \Lambda_2 = 2.5$, $N = 25$, $n_{th} = 100$, $\Gamma_{eff} = 0.126$, and $\gamma_s = 0.1$.

Figure 5 illustrates the impact of different dissipation rates on the dynamics of entanglement, highlighting the key role of dissipation processes in the generation of macroscopic quantum entanglement. The observations indicate that under conditions of lower dissipation rates, $\Gamma_{eff} = 0.120$, the system experiences less environmental dissipation, enabling the generation of stronger and more sustained entanglement. Conversely, at higher dissipation rates, environmental interference with the system increases, leading to a reduction in the purity of quantum states, thereby affecting the quality and duration of the entangled states. In this scenario, although the system can reach an entangled state, its entanglement performance significantly decreases, as indicated by the rise in the minimum value of the entanglement measure ξ. This phenomenon reveals the negative impact of dissipation dynamics on the capability of quantum information processing, especially in terms of the generation and maintenance of quantum entanglement. Dissipation processes typically accompany the loss of quantum information, reducing the system's potential for quantum entanglement. Therefore, in applications of quantum information science, controlling the interaction between the system and its environment is crucial, especially in the design of quantum communication, quantum computing, and other quantum technology schemes. By optimizing experimental and theoretical models to minimize environmentally induced dissipation, quantum entanglement can be effectively preserved and utilized, thereby enhancing the efficiency and reliability of quantum information processing.

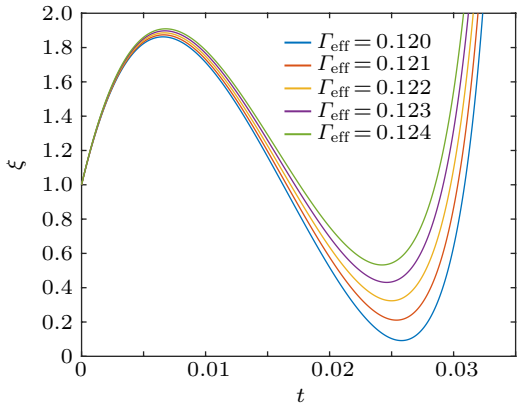


Fig. 5. Evolution of entanglement ξ over time with different parameters Γ_{eff}. The correlation parameters are $\lambda_1 = \lambda_2 = 0.1$, $\Lambda_1 = \Lambda_2 = 2.5$, $N = 25$, $n_{th} = 100$, $\Delta_s = 80$, and $\gamma_s = 0.1$.

4. Conclusion

In this study, we investigated the generation macroscopic quantum entanglement between two spin ensembles using an effective Hamiltonian of a coupled system based on SiV centers. The dynamic nature of macroscopic quantum entanglement and its sensitivity to various system parameters are examined. Specifically, we focus on the impact of parameters such as detuning Δ_s, decoherence rate γ_s, coupling constant λ_1, and environmental dissipation rate Γ_{eff} on the formation and maintenance of macroscopic quantum entanglement. Our findings indicate that increasing the detuning Δ_s can effectively prolong the duration of the entangled state and expedite the achievement of quantum entanglement within a shorter time frame. This demonstrates that macroscopic quantum entanglement can be controlled by adjusting the Δ_s parameter under suitable system conditions. Furthermore, we find that higher decoherence rates γ_s lead to decreased entanglement degree and shorter entanglement duration, highlighting the detrimental impact of environmental noise on entanglement generation and maintenance. Additionally, strong coupling (higher λ_1 values) is found to accelerate the entanglement formation process, while variations in the environmental dissipation rate Γ_{eff} significantly influence the quality and persistence of entanglement. It is well known that in the strong coupling regime, the interaction between the system and the environment is enhanced, leading to increased energy exchange and loss of coherence. This phenomenon is prevalent in quantum systems, where interaction with the environment (such as a thermal bath or other degrees of freedom) results in decoherence and energy dissipation, ultimately affecting entanglement. For instance, Breuer and Petruccione discussed the

role of environmental interactions in open quantum systems in their work, emphasizing how strong coupling enhances decoherence effects.[46] Similarly, Weiss provided comprehensive insights into dissipative quantum dynamics, highlighting how strong coupling leads to significant dissipation and coherence loss.[47] Specifically, in the strong coupling regime, the energy levels of the system are more susceptible to environmental fluctuations and noise, accelerating the decoherence rate. This is particularly detrimental to entangled states, which are highly sensitive to any perturbation. The decoherence and dissipation effects under strong coupling can significantly reduce the entanglement maintenance time, thereby limiting practical applications in quantum information processing and quantum computing. These results underscore the importance of precise control over system parameters for manipulating and harnessing quantum entanglement in quantum information technology. Future research could delve into the detailed mechanisms through which other parameters influence macroscopic quantum entanglement, advancing the development of quantum technologies.

Appendix A: Expectation of collective operators with time evolution

We outline the mean values that enter the variance of Eq. (13). As is known, for an operator O, the expectation with time evolution can be expressed by means of the master equation as $\mathrm{d}\langle O\rangle/\mathrm{d}t = \mathrm{tr}[O\dot{\rho}]$. Using Eq. (12), we can easily obtain the equations

$$\begin{aligned}
\frac{\mathrm{d}\langle J_{jx}\rangle}{\mathrm{d}t} &= (-1)^j\left(\frac{\Delta_\mathrm{s}}{2}+\frac{\lambda_j^2}{\Delta_\mathrm{s}}+\frac{\Lambda_j^2}{\Delta_\mathrm{s}}\right)\langle J_{jy}\rangle+(-1)^{j+1}\left(\frac{\lambda_j^2}{\Delta_\mathrm{s}}-\frac{\Lambda_j^2}{\Delta_\mathrm{s}}\right)\langle J_{jy}J_{jz}+J_{jz}J_{jy}\rangle\\
&\quad-\frac{2}{\Delta_\mathrm{s}}(\lambda_1\Lambda_2-\lambda_2\Lambda_1)\langle J_{jz}J_{iy}\rangle-\left(n_\mathrm{th}\Gamma_\mathrm{eff}+\frac{\Gamma_\mathrm{eff}}{2}\right)\langle J_{jx}\rangle+\frac{\Gamma_\mathrm{eff}}{2}\langle J_{jz}J_{jx}+J_{jx}J_{jz}\rangle-\frac{\gamma_\mathrm{s}}{2}\langle J_{jx}\rangle, \qquad \text{(A1)}\\
\frac{\mathrm{d}\langle J_{jy}\rangle}{\mathrm{d}t} &= (-1)^{j+1}\left(\frac{\Delta_\mathrm{s}}{2}+\frac{\lambda_j^2}{\Delta_\mathrm{s}}+\frac{\Lambda_j^2}{\Delta_\mathrm{s}}\right)\langle J_{jx}\rangle+(-1)^{j}\left(\frac{\lambda_j^2}{\Delta_\mathrm{s}}-\frac{\Lambda_j^2}{\Delta_\mathrm{s}}\right)\langle J_{jz}J_{jx}+J_{jx}J_{jz}\rangle\\
&\quad-\frac{2}{\Delta_\mathrm{s}}(\lambda_1\Lambda_2-\lambda_2\Lambda_1)\langle J_{ix}J_{jz}\rangle-\left(n_\mathrm{th}\Gamma_\mathrm{eff}+\frac{\Gamma_\mathrm{eff}}{2}\right)\langle J_{jy}\rangle+\frac{\Gamma_\mathrm{eff}}{2}\langle J_{jz}J_{jy}+J_{jy}J_{jz}\rangle-\frac{\gamma_\mathrm{s}}{2}\langle J_{jy}\rangle, \qquad \text{(A2)}\\
\frac{\mathrm{d}\langle J_{jz}\rangle}{\mathrm{d}t} &= \frac{2}{\Delta_\mathrm{s}}(\lambda_1\Lambda_2-\lambda_2\Lambda_1)\langle J_{jx}J_{iy}+J_{jy}J_{ix}\rangle-(2n_\mathrm{th}\Gamma_\mathrm{eff}+\Gamma_\mathrm{eff})\langle J_{jz}\rangle-\Gamma_\mathrm{eff}\langle J_{jx}^2+J_{jy}^2\rangle, \qquad \text{(A3)}\\
\frac{\mathrm{d}\langle J_{jz}J_{iy}\rangle}{\mathrm{d}t} &= (-1)^j\left(\frac{\Delta_\mathrm{s}}{2}+\frac{\lambda_i^2}{\Delta_\mathrm{s}}+\frac{\Lambda_i^2}{\Delta_\mathrm{s}}\right)\langle J_{jz}J_{ix}\rangle+(-1)^{j+1}\left(\frac{\lambda_i^2}{\Delta_\mathrm{s}}-\frac{\Lambda_i^2}{\Delta_\mathrm{s}}\right)\langle J_{jz}J_{iz}J_{ix}+J_{jz}J_{ix}J_{iz}\rangle\\
&\quad+\frac{2}{\Delta_\mathrm{s}}(\lambda_1\Lambda_2-\lambda_2\Lambda_1)\langle -J_{jz}J_{jx}J_{iz}+J_{jx}J_{iy}^2+J_{jy}J_{ix}J_{iy}\rangle-\frac{\gamma_\mathrm{s}}{2}\langle J_{jz}J_{jy}\rangle, \qquad \text{(A4)}\\
\frac{\mathrm{d}\langle C_{jzy}\rangle}{\mathrm{d}t} &= (-1)^{j+1}\left(\frac{\Delta_\mathrm{s}}{2}+\frac{\lambda_j^2}{\Delta_\mathrm{s}}+\frac{\Lambda_j^2}{\Delta_\mathrm{s}}\right)\langle C_{jxz}\rangle+(-1)^{j}\left(\frac{\lambda_j^2}{\Delta_\mathrm{s}}-\frac{\Lambda_j^2}{\Delta_\mathrm{s}}\right)\langle J_{jz}C_{jxz}+C_{jxz}J_{jz}\rangle\\
&\quad+\frac{2}{\Delta_\mathrm{s}}(\lambda_1\Lambda_2-\lambda_2\Lambda_1)\langle 2J_{jy}^2J_{ix}-2J_{jz}^2J_{ix}+C_{jxy}J_{iy}\rangle-\left(5n_\mathrm{th}\Gamma_\mathrm{eff}+\frac{5\Gamma_\mathrm{eff}}{2}\right)\langle C_{jzy}\rangle\\
&\quad-\frac{\gamma_\mathrm{s}}{2}\langle C_{jzy}\rangle+\frac{\Gamma_\mathrm{eff}}{2}\langle 2J_{jz}^2J_{jy}+2J_{jy}J_{jz}^2-4J_{jy}^3-J_{jx}C_{jxy}-C_{jxy}J_{jx}\rangle, \qquad \text{(A5)}\\
\frac{\mathrm{d}\langle C_{jxz}\rangle}{\mathrm{d}t} &= (-1)^j\left(\frac{\Delta_\mathrm{s}}{2}+\frac{\lambda_j^2}{\Delta_\mathrm{s}}+\frac{\Lambda_j^2}{\Delta_\mathrm{s}}\right)\langle C_{jzy}\rangle+(-1)^{j+1}\left(\frac{\lambda_j^2}{\Delta_\mathrm{s}}-\frac{\Lambda_j^2}{\Delta_\mathrm{s}}\right)\langle C_{jzy}J_{jz}+J_{jz}C_{jzy}\rangle\\
&\quad+\frac{2}{\Delta_\mathrm{s}}(\lambda_1\Lambda_2-\lambda_2\Lambda_1)\langle 2J_{jx}^2J_{iy}-2J_{jz}^2J_{iy}+C_{jxy}J_{ix}\rangle-(5n_\mathrm{th}\Gamma_\mathrm{eff}+\frac{5\Gamma_\mathrm{eff}}{2})\langle C_{jxz}\rangle\\
&\quad-\frac{\gamma_\mathrm{s}}{2}\langle C_{jxz}\rangle+\frac{\Gamma_\mathrm{eff}}{2}\langle -4J_{jx}^3-C_{jxy}J_{jy}+2J_{jz}^2J_{jx}+2J_{jx}J_{jz}^2-J_{jy}C_{jxy}\rangle, \qquad \text{(A6)}\\
\frac{\mathrm{d}\langle J_{jx}J_{iy}\rangle}{\mathrm{d}t} &= (-1)^j\left(\frac{\Delta_\mathrm{s}}{2}+\frac{\lambda_j^2}{\Delta_\mathrm{s}}+\frac{\Lambda_j^2}{\Delta_\mathrm{s}}\right)\langle J_{jy}J_{iy}\rangle+(-1)^j\left(\frac{\Delta_\mathrm{s}}{2}+\frac{\lambda_i^2}{\Delta_\mathrm{s}}+\frac{\Lambda_i^2}{\Delta_\mathrm{s}}\right)\langle J_{jx}J_{ix}\rangle\\
&\quad+\left(\frac{\lambda_j^2}{\Delta_\mathrm{s}}-\frac{\Lambda_j^2}{\Delta_\mathrm{s}}\right)\langle C_{jzy}J_{zy}\rangle+\left(\frac{\lambda_i^2}{\Delta_\mathrm{s}}-\frac{\Lambda_i^2}{\Delta_\mathrm{s}}\right)\langle J_{jx}C_{ixz}\rangle-\frac{2}{\Delta_\mathrm{s}}(\lambda_1\Lambda_2-\lambda_2\Lambda_1)\langle J_{jz}J_{iy}^2+J_{jx}^2J_{iz}\rangle\\
&\quad-(2n_\mathrm{th}\Gamma_\mathrm{eff}+\Gamma_\mathrm{eff})\langle J_{jx}J_{iy}\rangle+\frac{\Gamma_\mathrm{eff}}{2}\langle C_{jxz}J_{zy}+J_{jx}C_{izy}\rangle-\gamma_\mathrm{s}\langle J_{jx}J_{iy}\rangle, \qquad \text{(A7)}\\
\frac{\mathrm{d}\langle C_{jxy}\rangle}{\mathrm{d}t} &= (-1)^j2\left(\frac{\Delta_\mathrm{s}}{2}+\frac{\lambda_j^2}{\Delta_\mathrm{s}}+\frac{\Lambda_j^2}{\Delta_\mathrm{s}}\right)\langle J_{jy}^2-J_{jx}^2\rangle+(-1)^{j+1}\left(\frac{\lambda_j^2}{\Delta_\mathrm{s}}-\frac{\Lambda_j^2}{\Delta_\mathrm{s}}\right)\langle J_{jy}C_{jyz}+C_{jyz}J_{jy}-C_{jxz}J_{jx}-J_{jx}C_{jxz}\rangle\\
&\quad+\frac{2}{\Delta_\mathrm{s}}(\lambda_1\Lambda_2-\lambda_2\Lambda_1)\langle C_{jxz}J_{ix}+C_{jzy}J_{iy}\rangle-(2n_\mathrm{th}\Gamma_\mathrm{eff}+\Gamma_\mathrm{eff})\langle C_{jxy}\rangle
\end{aligned}$$

$$+\frac{\Gamma_{\rm eff}}{2}\left\langle J_{jx}C_{jzy}+C_{jzy}J_{jx}+J_{jy}C_{jxz}+C_{jxz}J_{jy}\right\rangle-2\gamma_{\rm s}\left\langle C_{jxy}\right\rangle, \tag{A8}$$

$$\begin{aligned}\frac{{\rm d}\left\langle J_{jy}^2\right\rangle}{{\rm d}t}=&(-1)^j\left(\frac{\Delta_{\rm s}}{2}+\frac{\lambda_j^2}{\Delta_{\rm s}}+\frac{\Lambda_j^2}{\Delta_{\rm s}}\right)\left\langle C_{jxy}\right\rangle-\frac{2}{\Delta_{\rm s}}(\lambda_1\Lambda_2-\lambda_2\Lambda_1)\left\langle J_{jzy}J_{ix}\right\rangle\\&+(-1)^j\left(\frac{\lambda_j^2}{\Delta_{\rm s}}-\frac{\Lambda_j^2}{\Delta_{\rm s}}\right)\left\langle J_{jy}C_{jxz}+C_{jxz}J_{jy}\right\rangle+(2n_{\rm th}\Gamma_{\rm eff}+\Gamma_{\rm eff})\left\langle J_{jz}^2-J_{jy}^2\right\rangle\\&+\frac{\Gamma_{\rm eff}}{2}\left\langle C_{jzy}J_{jy}+J_{jy}C_{jzy}\right\rangle-\gamma_{\rm s}\left\langle J_{jy}^2-J_{jx}^2\right\rangle,\end{aligned} \tag{A9}$$

$$\begin{aligned}\frac{{\rm d}\left\langle J_{jz}^2\right\rangle}{{\rm d}t}=&\frac{2}{\Delta_{\rm s}}(\lambda_1\Lambda_2-\lambda_2\Lambda_1)\left\langle C_{jxz}J_{iy}+J_{jzy}C_{ix}\right\rangle+2n_{\rm th}\Gamma_{\rm eff}\left\langle J_{jy}^2+J_{jx}^2\right\rangle-(4n_{\rm th}\Gamma_{\rm eff}+\Gamma_{\rm eff})\left\langle J_{jz}^2\right\rangle\\&+\frac{\Gamma_{\rm eff}}{2}\left\langle -C_{jxz}J_{jx}-J_{jx}C_{jxz}-C_{jzy}J_{jy}-J_{jy}C_{jzy}-2{\rm i}J_{jy}J_{jz}J_{jx}+2{\rm i}J_{jx}J_{jz}J_{jy}\right\rangle,\end{aligned} \tag{A10}$$

$$\begin{aligned}\frac{{\rm d}\left\langle J_{jx}^2\right\rangle}{{\rm d}t}=&(-1)^j\left(\frac{\Delta_{\rm s}}{2}+\frac{\lambda_j^2}{\Delta_{\rm s}}+\frac{\Lambda_j^2}{\Delta_{\rm s}}\right)\left\langle C_{jxy}\right\rangle-\frac{2}{\Delta_{\rm s}}(\lambda_1\Lambda_2-\lambda_2\Lambda_1)\left\langle J_{jxz}J_{iy}\right\rangle\\&+(-1)^{j+1}\left(\frac{\lambda_j^2}{\Delta_{\rm s}}-\frac{\Lambda_j^2}{\Delta_{\rm s}}\right)\left\langle J_{jx}C_{jzy}+C_{jzy}J_{jx}\right\rangle-(2n_{\rm th}\Gamma_{\rm eff}+\Gamma_{\rm eff})\left\langle J_{jx}^2-J_{jz}^2\right\rangle\\&+\frac{\Gamma_{\rm eff}}{2}\left\langle C_{jxz}J_{jx}+J_{jx}C_{jxz}\right\rangle-\gamma_{\rm s}\left\langle J_{jx}^2-J_{jy}^2\right\rangle,\end{aligned} \tag{A11}$$

$$\begin{aligned}\frac{{\rm d}\left\langle J_{1y}J_{2y}\right\rangle}{{\rm d}t}=&\left(\frac{\Delta_{\rm s}}{2}+\frac{\lambda_1^2}{\Delta_{\rm s}}+\frac{\Lambda_1^2}{\Delta_{\rm s}}\right)\left\langle J_{1x}J_{2y}\right\rangle-\left(\frac{\Delta_{\rm s}}{2}+\frac{\lambda_2^2}{\Delta_{\rm s}}+\frac{\Lambda_2^2}{\Delta_{\rm s}}\right)\left\langle J_{1y}J_{2x}\right\rangle-\left(\frac{\lambda_1^2}{\Delta_{\rm s}}-\frac{\Lambda_1^2}{\Delta_{\rm s}}\right)\left\langle C_{1xz}J_{2y}\right\rangle\\&+\left(\frac{\lambda_2^2}{\Delta_{\rm s}}-\frac{\Lambda_2^2}{\Delta_{\rm s}}\right)\left\langle J_{1y}C_{2xz}\right\rangle-\frac{2}{\Delta_{\rm s}}(\lambda_1\Lambda_2-\lambda_2\Lambda_1)\left\langle J_{1y}J_{1x}J_{2z}+J_{1z}J_{2x}J_{2y}\right\rangle-2(n_{\rm th}+\Gamma_{\rm eff})\left\langle J_{1y}J_{2y}\right\rangle\\&+\frac{\Gamma_{\rm eff}}{2}\left\langle C_{1zy}J_{2y}+J_{1y}C_{2zy}\right\rangle-\gamma_{\rm s}\left\langle J_{1y}J_{2y}\right\rangle,\end{aligned} \tag{A12}$$

$$\begin{aligned}\frac{{\rm d}\left\langle J_{1z}J_{2z}\right\rangle}{{\rm d}t}=&\frac{2}{\Delta_{\rm s}}(\lambda_1\Lambda_2-\lambda_2\Lambda_1)\left\langle J_{1z}J_{1x}J_{2y}+J_{1z}J_{1y}J_{2x}+J_{1x}J_{2y}J_{2z}+J_{1y}J_{2x}J_{2z}\right\rangle-4(n_{\rm th}+2\Gamma_{\rm eff})\left\langle J_{1z}J_{2z}\right\rangle\\&-\Gamma_{\rm eff}\left\langle J_{1x}^2J_{2z}+J_{1y}^2J_{2z}+J_{2x}^2J_{1z}+J_{2y}^2J_{1z}\right\rangle,\end{aligned} \tag{A13}$$

$$\begin{aligned}\frac{{\rm d}\left\langle J_{1x}J_{2x}\right\rangle}{{\rm d}t}=&-\left(\frac{\Delta_{\rm s}}{2}+\frac{\lambda_1^2}{\Delta_{\rm s}}+\frac{\Lambda_1^2}{\Delta_{\rm s}}\right)\left\langle J_{1y}J_{2x}\right\rangle+\left(\frac{\Delta_{\rm s}}{2}+\frac{\lambda_2^2}{\Delta_{\rm s}}+\frac{\Lambda_2^2}{\Delta_{\rm s}}\right)\left\langle J_{1x}J_{2y}\right\rangle+\left(\frac{\lambda_1^2}{\Delta_{\rm s}}-\frac{\Lambda_1^2}{\Delta_{\rm s}}\right)\left\langle C_{1zy}J_{2x}\right\rangle\\&-\left(\frac{\lambda_2^2}{\Delta_{\rm s}}-\frac{\Lambda_2^2}{\Delta_{\rm s}}\right)\left\langle J_{1x}C_{2zy}\right\rangle-\frac{2}{\Delta_{\rm s}}(\lambda_1\Lambda_2-\lambda_2\Lambda_1)\left\langle J_{1z}J_{2y}J_{2x}+J_{1x}J_{1y}J_{2z}\right\rangle-2(n_{\rm th}+\Gamma_{\rm eff})\left\langle J_{1x}J_{2x}\right\rangle\\&+\frac{\Gamma_{\rm eff}}{2}\left\langle C_{1xz}J_{2x}+J_{1x}C_{2xz}\right\rangle-\gamma_{\rm s}\left\langle J_{1x}J_{2x}\right\rangle,\end{aligned} \tag{A14}$$

where we define the covariance operator $\left\langle C_{jzy}\right\rangle=\left\langle J_{jy}J_{jz}+J_{jz}J_{jy}\right\rangle/2$, with $j,i=1,2$ $(j\neq i)$. Equations of motion including $\left\langle J_{jy}J_{iy}\right\rangle$, $\left\langle J_{jz}J_{iz}\right\rangle$, and $\left\langle J_{jx}J_{ix}\right\rangle$ provide the first-order (drift) terms in the partial differential equation, while equations of motion for symmetric-ordered operator pairs like $\left\langle C_{jzy}\right\rangle$ provide the second-order (diffusion) terms. Using the approximation $\langle J_k\mathcal{J}_sJ_p\rangle\approx\mathcal{J}_k\mathcal{J}_s\mathcal{J}_p+\mathcal{J}_kV_{sp}+\mathcal{J}_sV_{pk}+\mathcal{J}_pV_{ks}$ valid for Gaussian states. where $\mathcal{J}_s\equiv\langle\hat{J}_s\rangle$, $V_{nl}\equiv\frac{1}{2}\left\langle(\hat{J}_n-\mathcal{J}_n)(\hat{J}_l-\mathcal{J}_l)+(\hat{J}_l-\mathcal{J}_l)(\hat{J}_n-\mathcal{J}_n)\right\rangle$.[45]

Acknowledgements

Project supported by the National Natural Science Foundation of China (Grant No. 12265022), the Natural Science Foundation of Inner Mongolia Autonomous Region, China (Grant No. 2021MS01012), and the Inner Mongolia Fundamental Research Funds for the Directly Affiliated Universities (Grant No. 2023RCTD014).

References

[1] Horodecki R, Horodecki P, Horodecki M and Horodecki K 2002 *Rev. Mod. Phys.* **81** 865
[2] Mancini S, Giovannetti V, Vitali D and Tombesi P 2002 *Phys. Rev. Lett.* **88** 120401
[3] Dolde F, Jakobi I, Naydenov B, Zhao N, Pezzagna S, Trautmann C, Meijer J, Neumann P, Jelezko F and Wrachtrup J 2013 *Nat. Phys.* **9** 139
[4] Braunstein S L and van Loock P 2005 *Rev. Mod. Phys.* **77** 513
[5] Leggett A J and Garg A 1985 *Phys. Rev. Lett.* **54** 857
[6] Diósi L 1989 *Phys. Rev. A* **40** 1165
[7] Penrose R 1996 *Gen. Relat. Gravit.* **28** 581
[8] Amico L, Fazio R, Osterloh A and Vedral V 2008 *Rev. Mod. Phys.* **80** 517
[9] Tong X, Wang C, Cao C, He L and Zhang R 2014 *Opt. Commun.* **310** 166

[10] Yang Z B, Jin H, Jin J W, Liu J Y, Liu H Y and Yang R C 2021 *Phys. Rev. Res.* **3** 023126
[11] Cao C, Wang T J, Zhang R and Wang C 2015 *Laser Phys. Lett.* **12** 036001
[12] Ovartchaiyapong P, Lee K W, Myers B A and Jayich A C B 2014 *Nat. Commun.* **5** 4429
[13] Liu R, Liao Q, Zhao Q and Zhang Z 2023 *Eur. Phys. J. D* **77** 84
[14] Chotorlishvili L, Sander D, Sukhov A, Dugaev V, Vieira V R, Komnik A and Berakdar J 2013 *Phys. Rev. B* **88** 085201
[15] Zhou Y, Li B, Li X X, Li F L and Li P B 2018 *Phys. Rev. A* **98** 052346
[16] Muschik C A, Polzik E S and Cirac J I 2011 *Phys. Rev. A* **83** 052312
[17] Julsgaard B, Kozhekin A and Polzik E S 2001 *Nature* **413** 400
[18] Krauter H, Muschik C A, Jensen K, Wasilewski W, Petersen J M, Cirac J I and Polzik E S 2011 *Phys. Rev. Lett.* **107** 080503
[19] Feher G 1959 *Phys. Rev.* **114** 1219
[20] Xiang Z L, Ashhab S, You J Q and Nori F 2013 *Rev. Mod. Phys.* **85** 623
[21] Ma Y H, Ding Q Z and Yu T 2020 *Phys. Rev. A* **101**022327
[22] Li L, Schröder T, Chen E H, Walsh M, Bayn I, Goldstein J, Gaathon O, Trusheim M E, Lu M, Mower J, Cotlet M, Markham M L, Twitchen D J and Englund D 2015 *Nat. Commun.* **6** 6173
[23] Tchebotareva A, Hermans S L N, Humphreys P C, Voigt D, Harmsma P J, Cheng L K, Verlaan A L, Dijkhuizen N, De Jong W, Dréau A and Hanson R 2019 *Phys. Rev. Lett.* **123** 063601
[24] Toklikishvili Z, Chotorlishvili L, Mishra S K, Stagraczynski S, Schüler M, Rau A R P and Berakdar J 2017 *J. Phys. B: At. Mol. Opt. Phys.* **50** 055007
[25] Rittweger E, Wildanger D and Hell S W 2009 *Europhys. Lett.* **86**14001
[26] Naydenov B, Reinhard F, Lämmle A, Richter V, Kalish R, D'Haenens-Johansson U F S, Newton M, Jelezko F and Wrachtrup J 2010 *Appl. Phys. Lett.* **97** 242511
[27] Neumann P, Mizuochi N, Rempp F, Hemmer P, Watanabe H, Yamasaki S, Jacques V, Gaebel T, Jelezko F and Wrachtrup J 2008 *Science* **320** 1326
[28] Pfaff W, Taminiau T H, Robledo L, Bernien H, Markham M, Twitchen D J and Hanson R 2013 *Nat. Phys.* **9** 29
[29] Lemonde M A, Meesala S, Sipahigil A, Schuetz M J A, Lukin M D, Loncar M and Rabl P 2018 *Phys. Rev. Lett.* **120** 213603
[30] Chen J Q, Qiao Y F, Dong X L, Hei X L and Li P B 2021 *Phys. Rev. A* **103** 013709
[31] Ren Z Q, Lu X L and Xiang Z L 2024 *Opt. Express* **32** 4013
[32] Ren Z Q, Feng C R and Xiang Z L 2022 *Opt. Express* **30** 41685
[33] Hepp C, Müller T, Waselowski V, Becker J N, Pingault B, Sternschulte H, Steinmüller-Nethl D, Gali A, Maze J R, Atatüre M and Becher C 2014 *Phys. Rev. Lett.* **112** 036405
[34] Meesala S, Sohn Y I, Pingault B, Shao L, Atikian H A, Holzgrafe J, Gündoğan M, Stavrakas C, Sipahigil A, Chia C, Evans R, Burek M J, Zhang M, Wu L, Pacheco J L, Abraham J, Bielejec E, Lukin M D, Atatüre M and Lončar M 2018 *Phys. Rev. B* **97** 205444
[35] Qiao Y F, Li H Z, Dong X L, Chen J Q, Zhou Y and Li P B 2020 *Phys. Rev. A* **101**042313
[36] Fröhlich H 1950 *Phys. Rev.* **79** 845
[37] Nakajima S 1955 *Adv. Phys.* **4** 363
[38] Schrieffer J R and Wolff P A 1966 *Phys. Rev.* **149** 491
[39] Jing Y M, Alsina Daniel and Razavi Mohsen 2020 *Phys. Rev. Appl.* **14** 064037
[40] Sukachev D D, Sipahigil A, Nguyen C T, Bhaskar M K, Evans R E, Jelezko F and Lukin M D 2017 *Phys. Rev. Lett.* **119** 223602
[41] Bravyi S, DiVincenzo D P and Loss D 2011 *Ann. Phys.* **326** 2793
[42] Blais A, Gambetta J, Wallraff A, Schuster D I, Girvin S M, Devoret M H and Schoelkopf R J 2007 *Phys. Rev. A* **75** 032329
[43] Raymer M G, Funk A C, Sanders B C and De Guise H 2003 *Phys. Rev. A* **67** 052104
[44] Ma Y H, Ding Q Z and Wu E 2020 *Phys. Rev. A* **101** 022311
[45] Vardi A and Anglin J R 2001 *Phys. Rev. Lett.* **86** 568
[46] Breuer, Heinz-Peter and Francesco Petruccione 2010 *The Theory of Open Quantum Systems* (Oxford University Press)
[47] Weiss Ulrich 2012 *Quantum Dissipative Systems* (World Scientific)